Interferometric methods in diagnostics of polarization singularities

Oleg V. Angelsky, Igor I. Mokhun, Alexey I. Mokhun, and Marat S. Soskin
Chernivtsy University, Kotsybinsky Strasse, 2, Chernivtsy 12, 58012, Ukraine
(Received 15 March 2001; published 7 February 2002)

An interferometric technique for analysis of a polarization singular skeleton (*s* contours and *C* points) of an optical vector field is elaborated. It was shown that complete characteristics of *C* points and *s* contours may be reconstructed from interferometric data. Some examples of elaborated interferometric technique application to the analysis of randomly polarized speckle-fields singularities are presented.

DOI: 10.1103/PhysRevE.65.036602 PACS number(s): 42.25.−p

I. APPROACH TO THE PROBLEM

The problem of the analysis of zero-amplitude singular points and lines in two-dimensional (2D), lines and surfaces in 3D in optical fields (''singular optics'') has received great attention since 1974, when J. Nye and M. Berry had established and analyzed theoretically the existence of phase singularities of optical fields in the form of wave-front dislocations [1].

The set (system) of optical singularities may be considered as a peculiar skeleton of electromagnetic field [2–7,12–18]. In other words, the characteristics of optical singularities define the qualitative behavior of an electromagnetic field in its every point. The most complicated type of singularities is the polarization singularities intrinsic to vector fields [2–11].

To formulate precisely the problem of polarization singularities diagnostics of an optical vector field with arbitrary complexity, let us briefly overview the state-of-art of this problem for optical fields. The singularities of uniformly polarized fields represent common vortices, and they are described adequately by the scalar theory [19]. All of them can be identified and measured by the two-beam interferometry [19–23]. The variety of polarization singularities is wider [2]. There are two types of generic (stationary stable) singularities in the cross section of the propagating beam: (i) *s* contours—the closed loops with linear polarization of the electrical-field vector along them (the rotation direction of the field vector is indefinite), (ii) *C* points positioned in areas with left-hand polarization (LHP) or right-hand polarization (RHP) (the polarization azimuth is indefinite). *s* contours are the borders between the domains of LH and RH polarization. Each *C* point possesses a singularity index $I_c = \pm 1/2$. The sign of this index depends on the direction of rotation of ellipses located in the *C*-point vicinity during its path tracing in any direction. The index equals $+1/2$ or $-1/2$ if the axes rotate in the same direction or in the opposite direction [2]. There arises the problem of singular diagnostics of vector fields with variation from point to point.

It is well known that the measuring of field phase is very important for the investigation of characteristics of singularities in the scalar field. Of course, this also concerns polarization singularities. The measured polarization characteristics in the singularity points and in the closed areas under traditional polarimetry techniques may be practically indistinguishable. It is not possible to differentiate with absolute authenticity *s* contours (*C* points) and the field zones where elliptical polarization is close to the linear (circular) one.

Therefore, our task was to elaborate on the general interferometric technique for the polarization singularity diagnostics for an optical vector field. We also show here that the phase measurements may be important for polarization singularities.

The following approach was used to solve this task: (i) application of the known technique of ''fork'' interferometry [19–23] to the analysis of *s* singularities of arbitrary vector fields using their ''scalar'' linear-polarized projections with smoothly changeable azimuth from one projection to other; (ii) use of the known circular polarizer [24] for separation of the LHP circular orthogonal field component or the RHP one of a vector field.

II. THEORETICAL ANALYSIS AND EXPERIMENTAL PROCEDURE

A. Reconstruction of *s*-contour characteristics

Let us consider a vector field under paraxial approximation. The schematic view of such an optical field structure in some areas is presented in Fig. 1. The closed *s* contour and three *C* points inside it are shown. Let us decompose this vector field in the E_x, E_y components along the *X* and *Y* axes, correspondingly. We are sure that in the multitude of points of the *s* contour, there are the points, say *a* and *b*, in which the direction of electrical-field vibration is parallel to the *X* and *Y* axes, respectively, $E_x^{(a)} \neq 0$, $E_y^{(a)} = 0$, and $E_x^{(b)} = 0$, $E_y^{(b)} \neq 0$. Therefore, these points may be considered as the points where E_y, E_x components possess the wave-front dislocations correspondingly. To define their positions, it is enough to extract the component with wave-front dislocations by polarizer [2,11] and to organize the interference of this polarization projection with the same polarized reference beam. Rotation of the polarizer within the π limits gives the positions of all points of the *s* set. Note that the measurement accuracy of positions of *s* contour points does not depend considerably on the magnitude of intensity along *s*-contour in contrast to the conventional polarization measurements [10].

The direct *s*-contour diagnostics can be realized in the optical scheme presented in detail in Fig. 2.

The function of an analyzer *A* is twofold: (i) Separation of the linearly polarized projection of a vector field with the some azimuth for ''finding'' the corresponding points of *s*

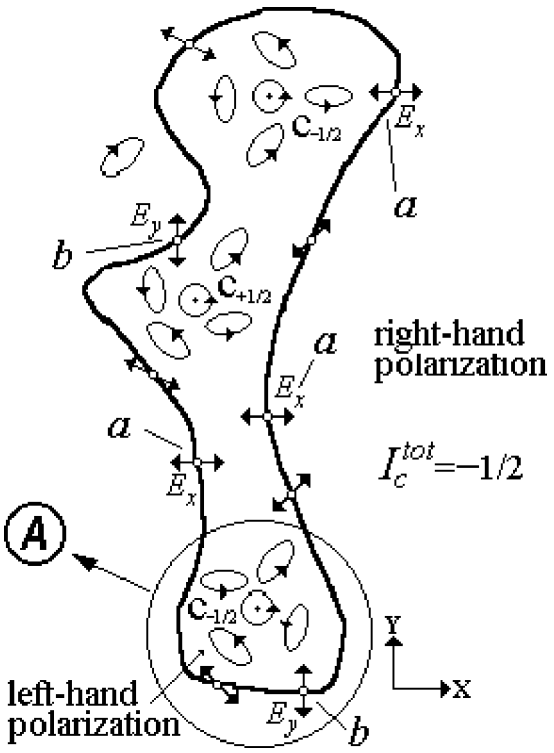

FIG. 1. Schematic view of typical realization of polarization singularities with closed *s* contour. There are three points (a) among the multitude of *s*-contour points, in which the field vibration is parallel to the *X* axis and two points (b), in which the vibration is polarized along the *Y* axis. All polarization ellipses inside *s* contour are left handed. Three left-hand circular polarized *C* points exist inside the *s* contour. Two of them possess a singular index $I_c=-1/2$, and the last one has an index $I_c=+1/2$. Therefore, the total singular index equals $I_c^{tot}=-1/2$. One outer right-hand polarized ellipse is also shown. The area *A* bounded by a circle will be used in Fig. 4 for a description of the elaborated technique.

contours as the zero-amplitude points. (ii) Selection of the same linearly polarized component from the circularly polarized reference beam to realize the off-axis interference. The zero-amplitude points will manifest themselves as branching points of interference fringes.

The results of some polarization speckle diagnostics are presented in Fig. 3. The analyzer was turned step by step on the 20^0 angle in the π interval and two-beam off-axis interferograms were fixed by a camera. Three selected situations

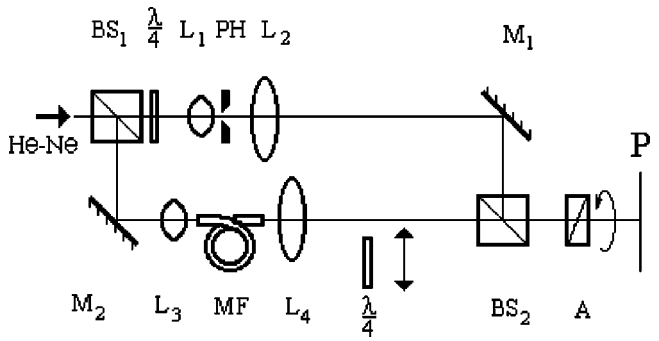

FIG. 2. Experimental setup for analysis of all stationary generic polarization singularities (*s* contours and *C* points). Linearly polarized light of He-Ne laser (633 nm) is launched into Mach-Zehnder interferometer with the upper reference and lower signal arms. BS_1 and BS_2 are beam splitters. 95% of laser energy is directed into the signal arm. BS_2 is the 50% beam splitter. M_1 and M_2 are the 100% mirrors. The $\lambda/4$ plate after BS_1 transforms the linearly polarized reference beam into a circular one. Objectives L_1 and L_2 and a pinhole PH form an expanded clean beam. $8^{\times}$ micro-objective L_3 launches linearly polarized laser beam into 10 cm multimode fiber MF. Objective L_4 forms the investigated polarization speckle field at the observation plane *P*. The front focal plane of L_4 coincides with the output end of the fiber. The far zone field is formed just after L_4. The additional $\lambda/4$ plate may be introduced in the objective arm for *C*-points analysis.

and the corresponding directions of analyzer azimuth are given in Figs. 3(a)–3(c). Figure 3(d) presents the result of the reconstruction of the closed *s* contour from interferometric measurements.

B. Interferometric technique for *C*-point identification

It seems from the first point of view, that the most direct way for *C*-point detection is intensity measurements by using a circular analyzer [24]. Then RHP *C* points would manifest as zero-amplitude points after the use of a left-hand circular analyzer and vice versa. But this simple procedure used by Hajnal [10] is effective only for relatively simple vector fields formed by the superposition of a limited number of plane waves. The analysis of the polarized speckle fields, where the local-field characteristics change smoothly and ''stochastically'' from point to point, is much more complicated. Indeed, there are extended dark areas in this field, but their intensity is nonzero. The existence of inevitable scat-

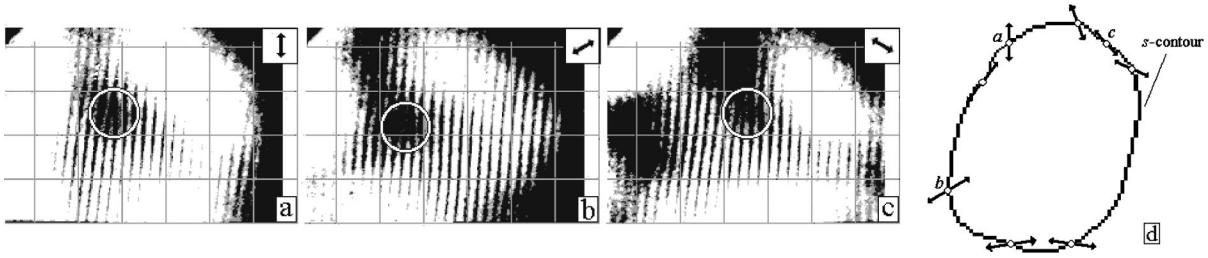

FIG. 3. The interferometric analysis of an *s* contour. (a)–(c) represent the ''fork'' interferograms. Orientations of the analyzer axis are shown in the upper-right corners. White circles mark the localization of *s* contour points. The reconstructed closed *s* contour is presented in Fig. 3(d).

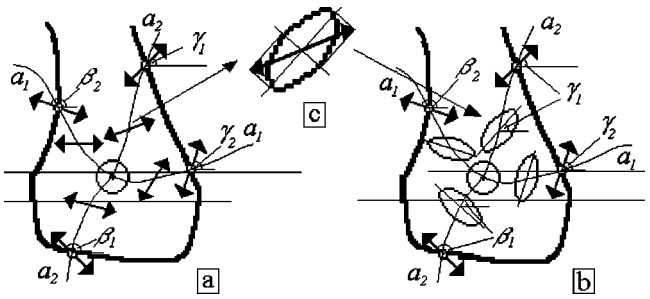

FIG. 4. Schematic view of part of the *s* contour shown in Fig. 1 (A area) with $C_{-1/2}$ point inside it. (a) Two equiazimuth lines a_1 and a_2 are formed by different orientation of λ/4 plate. Azimuths of linear polarization in the crossings of *a* lines (γ_1, γ_2, β_1, and β_2 correspondingly) and *s* contour coincide with the main directions of λ/4 plate for both orientations of it. (b) *a* lines are formed by the set of the ellipses with the same direction of major axis. When *a* lines cross *C* point, the chosen polarization azimuth γ_i changes on $\pi/2$ angle and transforms into azimuth β_i. (c) Reconstructed polarization ellipse in chosen point of a_2 line.

tered light from imperfections of optical scheme elements and scheme adjustment errors leads to additional difficulties for direct localization of *C* points in such a simple way.

We have elaborated a universal and precise interferomtric technique for the identification of *C* points in the direct way. To do this, an additional λ/4 plate is inserted into the setup after the fiber, as it is shown in Fig. 2. It transforms the elliptically polarized field into the linearly polarized one along some line, where the directions of the polarization ellipse axes coincide with the main directions of the inserted λ/4 plate. In other words, it ''selects'' from the sea of polarization ellipses in the area investigated the submultitude of ellipses with fixed azimuth, which degenerate into a line. As a consequence, other *s* contours are formed after the λ/4 plate. We will call the multitude of them the ''*azimuth lines*,'' or shortly, *a* lines. Note that the azimuth of linear polarization along the *a* line is defined by the ratio of axes magnitude of polarization ellipses in the same points of the field before passing the λ/4 plate. It is clear that rotation of the λ/4 plate will give an infinite family of such *a* lines. An absolute majority of them cross both the *s* contours and all *C* points inside it, because each *C* point and totality of *s* contour points possess all possible azimuths. Therefore, each *C* point represents itself as the *equiazimuth* star like each singular point in a scalar field is the *equiphase* star [1,13]. This nontrivial property is the key moment for the proposed technique. The schematic view of the part of the *s* contours presented in Fig. 1 surrounding one *C* point with an index $-1/2$ is shown in Fig. 4.

The *a* lines possess one peculiarity, which reminds us of the behavior of the equiphase lines, which execute π jump while crossing the singular point. Namely, the direction of the major polarization axis makes $\pi/2$ jump while crossing the C_i point [Figs. 4(a) and 4(b)]

$$\beta_i + \gamma_i = \pi/2, \tag{1}$$

where β_i, γ_i are the azimuths of polarization ellipses along a_i line.

Some properties of these lines are evident: (i) all *C* points have to be connected by all *a* lines, (ii) the chosen azimuth is defined by the azimuth of linear polarization in the point of *s* contour, which ''belongs'' to the given *a* line [see Fig. 4(a)]. It has been emphasized that these azimuths coincide with the given main directions of the λ/4 plate. The ratio of polarization ellipses axes (reconstruction of it) in some point of the *a* line may be easily obtained by the direct projection of the linearly polarized field vibration in this point on the main directions of the λ/4 plate [see Fig. 4(c)]. It is necessary for the determination of the singular indices for the found *C* points. To do this, we have to follow the rotation directions of major axes of at least three polarization ellipses in vicinity to *C* points during its path tracing [2].

To realize this technique, we have used a circular analyzer inserted in the signal arm with $\pi/4$ orientation of its axis in respect to the direction of the *A* analyzer's axis. Such experimental arrangement allows us to visualize *C* points in areas, for example, with the right-hand polarization. That is possible due to the formation of wave-front dislocations in *C* points in the polarization projection after analyzer *A*. Rotation of the λ/4 plate (or analyzer *A*) on the $\pm\pi/2$ angle leads to visualization of *C* points in the areas with left-hand polarization. Note that simultaneous rotation of the λ/4 plate and the analyzer *A* on any angle leaves the polarization projection without changes. Rotation of the analyzer *A* on some angle (orientation of the λ/4 plate remains unchanged), which differs from $\pm\pi/2$ leads to a shift of the vortices along *a* lines separated by orientation of the λ/4 plate. Vortices move towards the other *C* point, cross it when a rotation angle is equal to $\pm\pi/2$. Of course, such vortex motion may be identified as the corresponding one of an interference fork. Change of orientation of the λ/4 plate leads to vortex motion along *a* lines with other azimuths. Thus, the family of

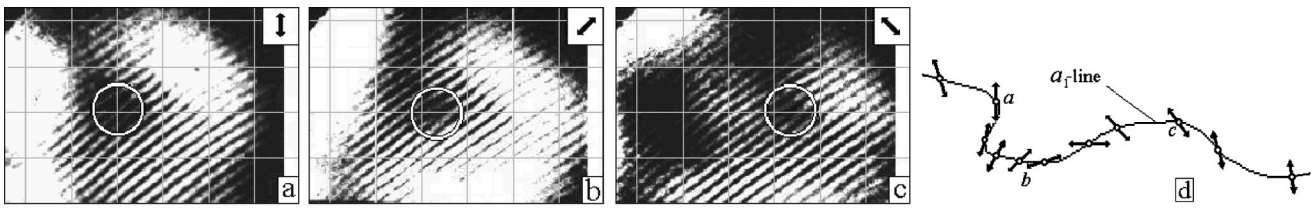

FIG. 5. (a)–(c) are selected ''fork'' interferograms for an analyzer angles, which are equal to 0^0, 45^0, and 135^0; (d) Represents a piece of the reconstructed a_1 line.

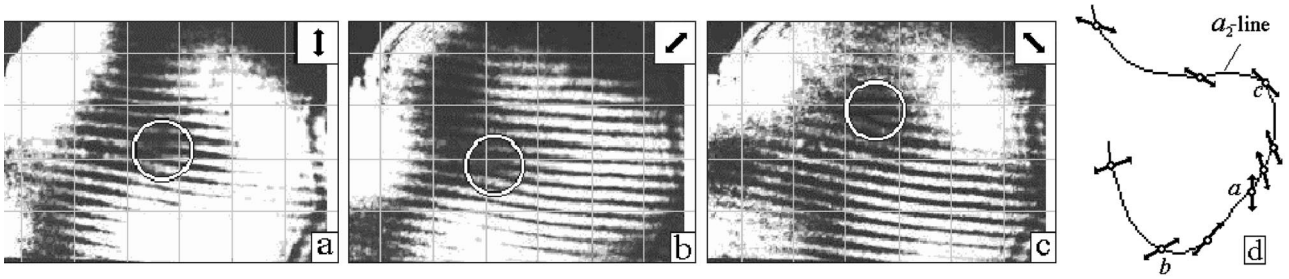

FIG. 6. (a)–(c) are selected ''fork'' interferograms for analyzer angles, which are equal to 0^0, 45^0, and 135^0; (d) Represents a piece of the reconstructed a_2 line.

a lines (for example, lines a_1 and a_2 in Fig. 4) may be obtained.

The determined equiazimuth lines $a1$ and $a2$ needed for *C* points' identification together with the some fork interferograms are presented in Figs. 5 and 6, correspondingly. The interferograms were fixed for an analyzer orientation angle changed steplike with a 20^0 interval. When azimuth of an analyzer is changed, the branching points of interference forks trace two various *a* lines, which obligatorily intersect in *C* points.

An example of the identification of chosen *C* points is presented in Fig. 7. It can be seen from Fig. 7(b) that polarization ellipses rotate in the opposite direction to the direction of path tracing, i.e., the singular index of considered *C* points equals $I_c = -1/2$.

The elaborated technique possesses much more general sense than the measurement of the singular field skeleton only, because it allows us to measure all characteristics of a polarization ellipse in each point (p) of vector field. To do this, we need to make the following manipulations: (i) to reconstruct the *s* contours (intrinsic to the investigated area of a field) initially without the $\lambda/4$ plate in the signal arm; (ii) to insert the $\lambda/4$ plate and to find the *a* line, which goes through this point; (iii) to measure azimuth φ_1 for the corresponding *s* contour point by the analyzer *A*; it gives the orientation of the polarization ellipse major axis; (iv) to measure azimuth φ_2 by the analyzer *A* when the interference fork reaches this very point (p). Then, the investigated ellipse possesses the major axis with azimuth φ_1 and ellipticity is defined by the angle φ_2. The measured characteristics give in totality all parameters of the polarization ellipse under investigation, namely, the orientation of ellipse axes and the ratio of their magnitudes.

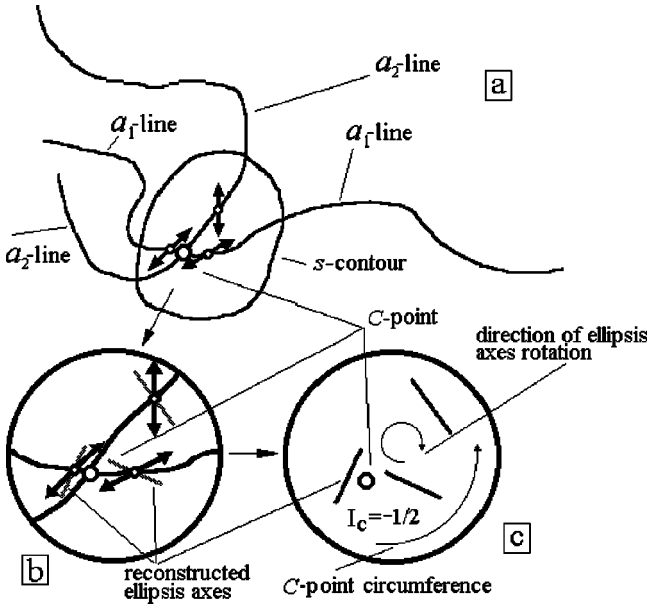

FIG. 7. (a) Represents the general arrangement of *s* contour, *C* point inside it and two equiazimuth lines a_1 and a_2. The detailed structure of orientations of polarization ellipses' major axes in the *C*-point vicinity is shown in large scale in circles (b) and (c), respectively. (b) Represents the orientation of linear polarization azimuth of three chosen points on a_1 and a_2 lines. (c) Shows direction of rotation of polarization axes during *C*-point path tracing.

The elaborated technique possesses the self-dependent value for the broad field of important polarimetric problems. The investigation with high-space resolution of polarization structure in the low-intensity areas may be an example of it. This is urgent for the investigation of vector fields formed by ''weak-depolarizing'' scatterers, because the ''damage'' of primary polarization takes place in these areas.

The obtained experimental results are a successful attempt of the complete analysis of fine singular structure of irregular optical vector speckle field.

III. CONCLUSION

Two-beam interferometric technique, or space phaseometry, for the diagnostics of all types of the polarization field singularities (characteristics of *s* contours and *C* points) has been elaborated. It is based on transformation of the elliptical polarization into the linear one with any azimuth, which can be defined with high preciseness. In this way, this operation reduces the problem of a vector field analysis to the analysis of the totality of scalar field realizations. It is elaborated in detail and is based on well-known ''fork'' interferometry. The equiazimuth lines have been introduced for singularity analysis. Their parameters and crossing points define the position of *C* points with circular polarization and their singular indices. The elaborated technique enables us to measure all actual characteristics of a polarization ellipse in each point of a vector field. The experimental setup is described. The example of the determination of the polarization speckle-field's singular skeleton is presented.

[1] J. F. Nye and M. V. Berry, Proc. R. Soc. London, Ser. A **336**, 165 (1974).
[2] J. F. Nye, *Natural Focusing and Fine Structure of Light* (Institute of Physics Publishing, Bristol, 1999).
[3] J. F. Nye, Philos. Trans. R. Soc. London, Ser. A **355**, 2065 (1997).
[4] J. F. Nye, Philos. Trans. R. Soc. London, Ser. A **387**, 105 (1983).
[5] J. F. Nye and J. V. Hajnal, Philos. Trans. R. Soc. London, Ser. A **409**, 21 (1987).
[6] J. F. Nye, Proc. R. Soc. London, Ser. A **389**, 279 (1983).
[7] J. V. Hajnal, Proc. R. Soc. London, Ser. A **414**, 433 (1987).
[8] J. V. Hajnal, Proc. R. Soc. London, Ser. A **414**, 447 (1987).
[9] J. V. Hajnal, Proc. R. Soc. London, Ser. A **430**, 413 (1990).
[10] J. V. Hajnal, Ph.D. theses, University of Bristol, 1985.
[11] O. Angelsky, R. Besaha, A. Mokhun, I. Mokhun, M. Sopin, and M. Soskin, Proc. SPIE **3904**, 40 (1999).
[12] I. Freund and N. Shvartsman, Phys. Rev. A **50**, 5164 (1994).
[13] I. Freund, N. Shvartsman, and V. Freilikher, Opt. Commun. **101**, 247 (1993).
[14] I. Freund and N. Shvartsman, Opt. Commun. **117**, 228 (1995).
[15] I. Freund and N. Shvartsman, Phys. Rev. Lett. **72**, 1008 (1994).
[16] I. Freund, Proc. SPIE **2389**, 411 (1995).
[17] I. Fruend, Phys. Rev. E **52**, 2348 (1995).
[18] I. Fruend, J. Opt. Soc. Am. A **14**, 1911 (1997).
[19] N. B. Baranova, B. Ya. Zel'dovich, A. V. Mamayev, N. F. Pilipetsky, and V. V. Shkunov, Zh. Éksp. Teor. Fiz. **33**, 1779 (1981) [Sov. Phys. JETP **33**, 1789 (1981)].
[20] A. G. White, C. P. Smith, N. R. Heckenberg, H. Rubinsztein-Dunlop, R. McDuff, C. O. Weiss, and Chr. Tamm, J. Mod. Opt. **38**, 2531 (1991).
[21] V. Yu. Bazhenov, M. V. Vasnetsov, and M. S. Soskin, Pis'ma Zh. Éksp. Teor. Fiz. **52**, 431 (1990) [JETP Lett, **52**, 429 (1990)].
[22] I. V. Basistiy, M. V. Vasnetsov, and M. S. Soskin, Opt. Commun. **119**, 604 (1995).
[23] N. R. Heckenberg, R. McDuff, C. P. Smith, H. Rubinsztein-Dunlop, and M. J. Wegener, Opt. Quantum Electron. **24**, S951 (1992).
[24] M. Born and E. Wolf, *Principles of Optics*, 6th ed. (Pergamon Press, Oxford, 1987).